

Tunable Luminescent Lanthanide Supramolecular Assembly Based on Photoreaction of Anthracene

Yan Zhou,[†] Heng-Yi Zhang,^{†,‡} Zhi-Yuan Zhang,[†] and Yu Liu^{*,†,‡,‡}

[†]Department of Chemistry, State Key Laboratory of Elemento-Organic Chemistry, Nankai University, Tianjin 300071, P. R. China

[‡]Collaborative Innovation Center of Chemical Science and Engineering (Tianjin), Tianjin 300071, P. R. China

S Supporting Information

ABSTRACT: Lanthanide luminescence materials generally show great superiority in light-emitting materials, gaining increasingly exploration in the design of advanced functional materials. Herein, we prepared a supramolecular assembly via the coordination of a host molecule (**1**) and dilanthanide metal. Compound **1** possesses a 9,10-diphenylanthracene (ant) core with photosensitivity and terminal terpyridine (tpy), containing two-arm dibenzo-24-crown-8. The assembly could exhibit excellent lanthanide luminescence after undergoing a photoreaction from anthracene unit in **1**. Significantly, the luminescence of the assembly could be reversibly switched on and off through a regulable photoreaction upon light irradiation or heating. The multiple functional behavior combined with the ease of assembly reveals that this photo/thermo-controlled lanthanide luminescence supramolecular polymer design method offers a convenient pathway for future engineering of multi-stimuli-responsive materials.

Rapidly growing research on stimuli-responsive smart materials has implications for the development of drug nanocarriers,¹ optical switches,² data storage,³ optoelectronic devices,⁴ functional vesicles,⁵ super-resolution imaging,⁶ and molecular machines.⁷ Among the various functional devices, lanthanide-luminescence-based ones are being increasingly explored in the design of advanced functional materials because of their unique luminescence properties, such as long-lived excited states, sharp line-like emission bands, and large Stokes shifts.⁸ Within the past decade or so, a number of important breakthroughs have been made in the development of lanthanide-doped nanoparticles.⁹ The most intriguing emission property of lanthanide doped nanophosphors is the up-conversion luminescence, which have been mainly used in the area of optical devices,¹⁰ and some of them show considerable promise for the biomedical applications.¹¹ Hence, the lanthanide luminescent materials would be a truly viable choice as active materials for optoelectronic and sensing devices. With the rapid development of the lanthanide materials, the reversible modulation of the luminescent intensity of lanthanide complexes becomes one of the most attractive aims in molecular switches.¹² We were also interested in constructing several supramolecular devices including tris[2]-pseudorotaxane¹³ and [2]pseudorotaxane,¹⁴ and demonstrated that they are the excellent reversible luminescent lanthanide molecular switches in the presence of K⁺ or 18-crown-6 (18C6). Despite

a variety of research efforts in designing the smart devices for regulating the luminescence of lanthanide complexes, more attention has been paid on the single molecule devices, and designing the reversible stimuli-responsive luminescent dilanthanide supramolecule assembly switches upon a regulable photoreaction remain a considerable challenge. We herein prepared a supramolecular assembly via the coordination of a new host molecule (**1**) and dilanthanide metal. We introduced a 9,10-diphenylanthracene (ant) in **1** as a photoresponsive group, which makes the lowest triplet state of ligand **1** match with the first excited lanthanide state after undergoing photo-oxygenation of ant group. We also introduced two terpyridine (tpy) groups as a chelating ligand to coordinate with Tb³⁺ and Eu³⁺ ions. In addition, the existence of two crown ether rings is to prevent the influence of alkali and alkaline earth metal ions on luminescence of the Ln³⁺. The assembly could exhibit excellent lanthanide luminescence after undergoing a photoreaction from anthracene unit in **1**. Moreover, control of the photo-oxygenation process upon light or heat as inputs enabled the reversible on/off switching of the lanthanide luminescence.

The syntheses of **1** and the reference compounds **2** and **3** are shown in the Supporting Information, and structures are presented in Figure 1). Briefly, the **1** was prepared in 60% yield

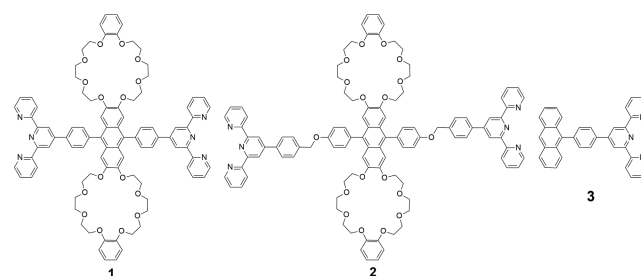


Figure 1. Structures of host compound **1**, reference compounds **2** and **3**.

by the Suzuki reaction of 9,10-dibromoanthracene-DB24C8 derivative with (4-([2,2':6',2''-terpyridin]-4'-yl)phenyl)boronic acid under basic conditions, while compounds **2** and **3** were prepared in 42% and 88% yield, respectively, according the similar synthesis method to **1**.

Building upon our previous work on luminescent supramolecular devices,^{13,14} we sought to incorporate the equimolar

Received: March 29, 2017

Published: May 16, 2017

Tb³⁺ and Eu³⁺ ions into **1** in CHCl₃/CH₃CN (1:1, v/v). It is strange that the unique emission properties of Ln³⁺ ions were not observed, and the fluorescence of **1** was quenched (Figure 2a). As we all known, the terpyridine group is an excellent

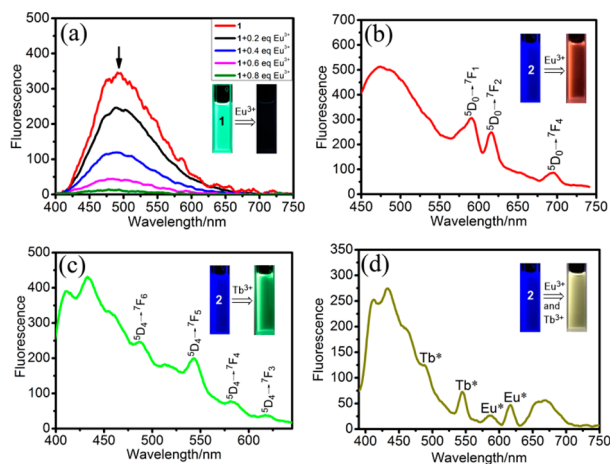


Figure 2. Emission spectra variation of (a) **1** ([**1**] = 0.01 mM) upon addition of Eu³⁺ or Tb³⁺ ($\lambda_{\text{ex}} = 365$ nm), (b) Eu-2, (c) Tb-2, and (d) EuTb-2 ($\lambda_{\text{ex}} = 290$ nm) ([**2**] = 0.01 mM). Inset photo image of fluorescence changes of **1** and **2** upon addition of Eu³⁺ or Tb³⁺ in CH₃CN/CHCl₃ (1:1, v/v) solution.

sensitizer for lanthanide ions, especially Eu³⁺ and Tb³⁺ ions.¹⁵ So, we speculate that the synthetic host molecule contains a large aromatic conjugation system, leading to the properties of the terpyridine group vary drastically compared with simple terpyridine group, resulting in a mismatch between the lowest triplet state of ligand **1** and the first excited lanthanide state. It means that the host molecule **1** cannot be used as an efficient sensitizer.¹⁶ As a result, there is no emission properties of Ln³⁺ by addition of Ln³⁺ into **1**. Moreover, the Job analysis of the fluorescence spectral data (Figure S18) gave the stoichiometric 1:1 binding ratio between **1** and Eu³⁺ ion. Direct morphological information was provided by transmission electron microscopy (TEM) observations, showing that compound **1** was the small nanoparticle morphology (Figure S19a). On the basis of the TEM analysis, the average diameters of the **1** nanoparticles are about 15 nm. When we added Eu³⁺ and Tb³⁺ into **1**, the resultant Ln-**1** complexes formed spherical nanoparticles (Figure S19b). On the basis of the TEM analysis, the average diameters of the Ln-**1** spherical nanoparticles are about 170 nm. The DLS results demonstrated that the main size distribution of the **1**/Eu³⁺ system was ca. 240 nm, which was basically consistent with the microscopic investigation results (Figure S19c). In addition, ¹H NMR spectra of host **1** showed that, after the addition of 1.2 equiv of Eu(OTf)₃, the aromatic H_{Ar} protons of tpy moiety were shifted upfield and downfield, with a serious passivation, whereas the H_{ethyl} protons of ethyl groups in DB24C8 ring also changed correspondingly (Figure S20). These results jointly demonstrated that Eu³⁺ was coordinated with **1** to form metal-ligated species. The crown ether rings, meanwhile, had some complexing capacities with Eu³⁺.

It is well-documented that anthracenes are photoresponsive and transform into dimerization under UV light irradiation.¹⁷ In addition, anthracene can also trap singlet oxygen and form stable endoperoxides (EPOs),¹⁸ which the process is reversible and the reverse process can be actuated under thermolysis. If there are substituent groups in the 9,10-positions of anthracene,

especially alkynyl-substituted or aryl-substituted groups, it tends to undergo a photo-oxygenation process. EPOs of anthracenes can be obtained by the [4+2]-cycloaddition with ¹O₂. The large substituent groups in the 9,10-positions of anthracene cause steric hindrance for photodimerization and favor photo-oxygenation. We envisaged that the anthracene unit in **1** will react rapidly to the corresponding EPO after UV light irradiation.

To testify this presumption, the host molecule **1** was first irradiated at 365 nm under N₂ atmosphere. Its ¹H NMR spectrum showed no obvious changes after 1 h of irradiation, indicating that the steric hindrance caused by the phenyl groups in the 9,10-positions of anthracene prevented from photodimerization (Figure S28). When **1** was irradiated at 365 nm in the presence of O₂, the corresponding EPO product was undoubtedly obtained. Accordingly, UV-vis absorption measurements, fluorescence spectrum, MALDI-TOF-MS, and ¹H NMR were performed to monitor the photo-oxygenation process of anthracene. The absorption of the anthracene moiety in the range of 350–420 nm vanished completely after irradiation by UV light at 365 nm for 100 s, implying that the anthracene chromophore had quantitatively been changed (Figure S29a). Comparatively, the corresponding emission spectra of **1** ($\lambda_{\text{ex}} = 365$ nm) showed a decrease in intensity at 500 nm with the concomitant appearance of peak at 428 nm after 100 s of irradiation at 365 nm, indicating that the anthracene chromophore photoreacted (Figure S29b). ¹H NMR spectroscopy is a powerful tool to determine the reversible photo-oxygenation process. As shown in Figure 4, the proton signals of H^a at 6.82 ppm assigned to the protons of ant group in **1** displayed a upfield shift after UV light irradiation ($\lambda_{\text{irr}} = 365$ nm, $t_{\text{irr}} = 100$ s). While the proton signals of H^b at 7.61 ppm assigned to the protons of benzene in tpy group displayed a downfield shift. These results indicated the conversion of ant group to EPO one. In addition, when the EPO was heated at 50 °C for 30 h, a full reconversion to the parent species **1** occurred, as confirmed by ¹H NMR spectroscopy (Figure 3d). Moreover, MALDI-TOF-MS was performed to monitor the photo-oxygenation process (Figure S30). By these results, we confirmed that the ant core within the host molecule could undergo reversible photooxygenation between ant (thermolysis) and EPO ($\lambda = 365$ nm irradiation), which can be utilized for further functional explorations.

The above results suggested that host molecule could retain partial structural integrity upon UV-triggered ant-to-EPO transition (Figure 3). The EPO-form host molecular, arisen from UV irradiation with O₂, still contains terminal tpy groups. Therefore, **1**_{EPO} would be combined with Ln³⁺ ion to afford a metallosupramolecular assembly. Interaction of **1**_{EPO} with Eu³⁺ ions was studied in CHCl₃/CH₃CN (1:1, v/v) solution by adding Eu³⁺ to **1**_{EPO} with a tpy:Eu³⁺ ratio of 2:1. Benefiting from the excellent luminescence properties of Eu³⁺, complex Eu-**1**_{EPO} displayed satisfactory luminescence in solution. When excited at 320 nm, the complex showed five sharp emission peaks, at 541 nm (⁵D₀→⁷F₀), 590 nm (⁵D₀→⁷F₁), 615 nm (⁵D₀→⁷F₂), 648 nm (⁵D₀→⁷F₃), and 684 nm (⁵D₀→⁷F₄) (Figure 4a). The fluorescence of Eu-**1**_{EPO} may be attributed to intramolecular energy transfer (ET) from the excited tpy moiety to Eu³⁺.

Similar changes in fluorescence spectra were also observed in the case of Tb³⁺ ion. The emission spectra of Tb-**1**_{EPO} exhibited sharp bands at 489, 544, 584, and 620 nm (Figure 4b). They were assigned to the ⁵D₄→⁷F₆, ⁵D₄→⁷F₅, ⁵D₄→⁷F₄, and

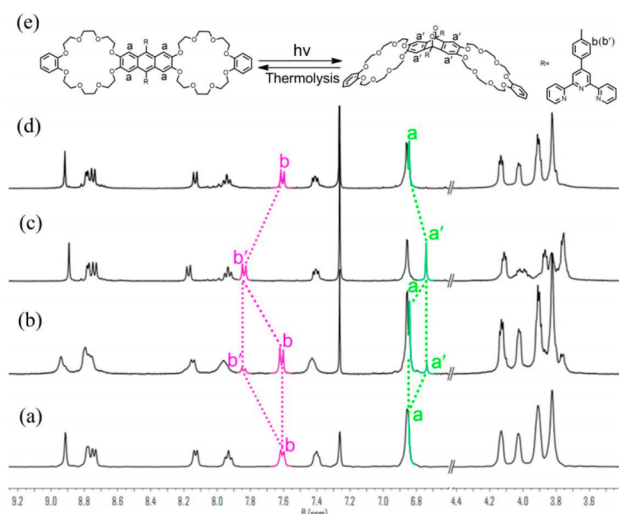


Figure 3. ^1H NMR spectra monitoring the reversible photo-oxygenation of **1** ($[\mathbf{1}] = 1 \text{ mM}$): (a) before irradiation with UV light, (b) after irradiation 20 s at 365 nm, (c) after irradiation 100 s at 365 nm, (d) after irradiation at 365 nm for 100 s and heating at 50 °C for 30 h, and (e) reversible structural transformation of **1** by irradiation at 365 nm and heating.

$^5\text{D}_4 \rightarrow ^7\text{F}_3$ transition of Tb^{3+} , respectively. The quantum yield (QY) upon excitation at 320 nm was 12.4% for $\text{Eu}\cdot\mathbf{1}_{\text{EPO}}$ and 4.2% for $\text{Tb}\cdot\mathbf{1}_{\text{EPO}}$, suggesting that the luminescence of the assembly could be modulated by a photoreaction. Moreover, when equimolar Tb^{3+} and Eu^{3+} ions were simultaneously added into $\mathbf{1}_{\text{EPO}}$, the bimetallic $\text{EuTb}\cdot\mathbf{1}_{\text{EPO}}$ showed strong pale-yellow-emissive (Figure 4c). With the help of their luminescent properties, we determined the stoichiometry of Tb versus Eu in $\text{EuTb}\mathbf{1}_{\text{EPO}}$ by integrating the Tb^{3+} ($^7\text{F}_6$) and the Eu^{3+} ($^7\text{F}_4$) transitions,¹⁹ and the obtained value of Tb:Eu is about 4:1. We also further explored the morphological information on the $\text{Ln}\cdot\mathbf{1}_{\text{EPO}}$ nanoarchitecture using TEM observations. The complex $\text{Ln}\cdot\mathbf{1}_{\text{EPO}}$ revealed the nanofibrous morphology (Figure S31), whereas the spherical nanoparticles were also found, indicating a possible secondary aggregation of linear assemblies into spheres by the coiling. We also embedded the $\text{Ln}\cdot\mathbf{1}_{\text{EPO}}$ complexes into poly(methyl methacrylate) (PMMA). The spin-coated films were found to exhibit excellent and characteristic lanthanide luminescence in the solid state similar to that observed in solution (Figures S32 and S33), indicative of utmost importance to their practical applications. Intriguingly, the existence of crown ether ring in this system could effectively prevent the influence of alkali and alkaline earth metal ions on luminescence of Ln^{3+} , especially for Ba^{2+} (Figure S34). To some extent, the fluorescence intensity of Ln^{3+} increased obviously after adding the alkali and alkaline earth metal ions. The results suggested that the existence of crown ether ring in this system could bind with the alkali and alkaline earth metal ions, which may lead to the structure immobilization of the supramolecular assembly, accompanied by an increase of the rigidity of the assembly, which jointly cause an increase of the fluorescence intensity of $\text{Ln}\cdot\mathbf{1}_{\text{EPO}}$. Furthermore, we synthesized one reference compound **2** with a non-conjugation link between ant and tpy, and one terminal terpyridine compound **3**. The control experiments using **2** and **3** were performed, respectively. The results obtained indicate that there exists the intramolecular energy transfer (ET) from the excited terpyridine moiety of **2** or **3** to Ln^{3+} ,²⁰ leading to

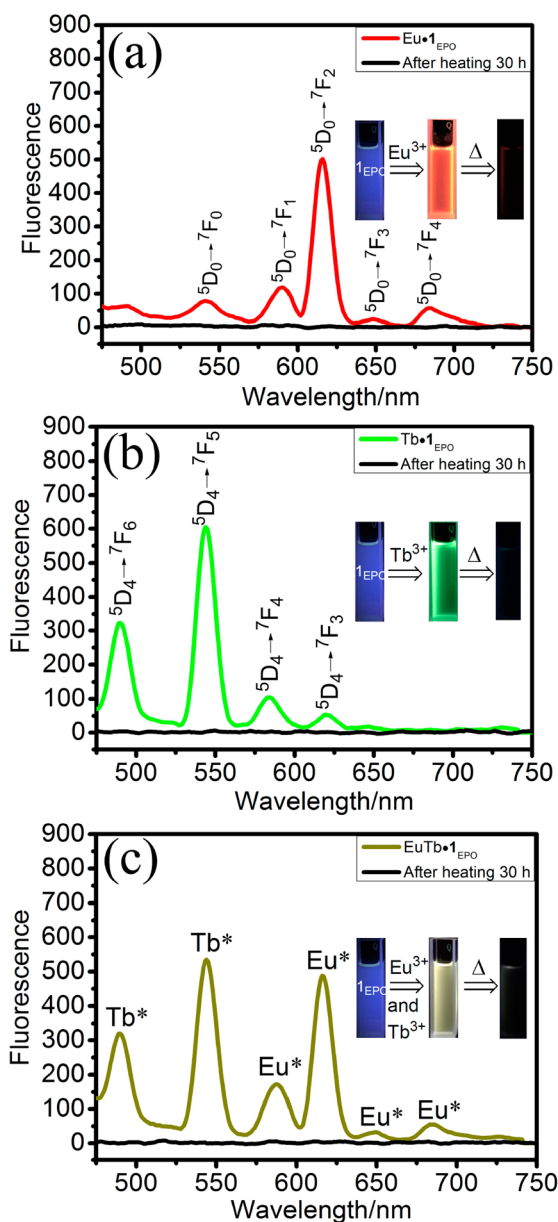
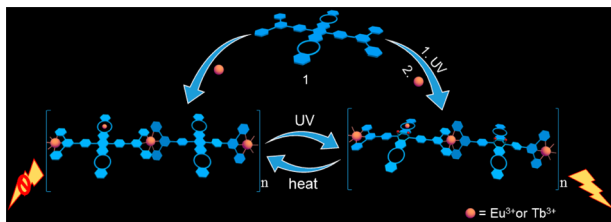


Figure 4. Emission spectra of (a) $\text{Eu}\cdot\mathbf{1}_{\text{EPO}}$, (b) $\text{Tb}\cdot\mathbf{1}_{\text{EPO}}$, (c) $\text{EuTb}\cdot\mathbf{1}_{\text{EPO}}$ and emission intensity changes after heating 30 h ($\lambda_{\text{ex}} = 320 \text{ nm}$). Inset photo image of fluorescence changes of $\mathbf{1}_{\text{EPO}}$ upon addition of Eu^{3+} or Tb^{3+} in $\text{CH}_3\text{CN}/\text{CHCl}_3$ (1:1, v/v) solution, and then heating 30 h.

neither Ln-2 nor Ln-3 being used to switch on/off the luminescence. Therefore, it is necessary to design both a conjugation system of ant with tpy and the dilanthanide metal poly complex.

The reversible photo-oxygenation process of anthracene unit in **1** further enabled us to modulate the luminescence of the assembly. Intriguingly, as shown in Figure 4, the characteristic fluorescence emission of the assembly was significantly quenched upon EPO-to-ant transition after heating the $\text{Ln}\cdot\mathbf{1}_{\text{EPO}}$ for 30 h. Briefly, the supramolecular assembly could exhibit the expected luminescent lanthanide switching behavior through reversible ant-to-EPO transition. Scheme 1 shows the switch modes of the assembly, which exhibits the expected luminescent lanthanide switching behavior.

Scheme 1. Schematic Illustration of the Lanthanide Luminescence Driven by the Process of Reversible Photoreaction



In summary, a photoreaction tunable reversible lanthanide luminescence supramolecular assembly was successfully constructed through the host molecule **1** and lanthanide metal. Significantly, the existence of crown ether ring in this system could effectively prevent the influence of alkali and alkaline earth metal ions on luminescence of the Ln·I_{EPO}, and the lanthanide luminescence of assembly could be reversibly responsive through a regulable photoreaction upon light irradiation or heating. The photo/thermo-stimuli-driven luminescent lanthanide molecular switch augurs well for their future in multi-stimulus-driven molecular machines and logic gates applications.

■ ASSOCIATED CONTENT

Supporting Information

The Supporting Information is available free of charge on the ACS Publications website at DOI: 10.1021/jacs.7b03153.

Compound characterization, and additional figures in the optical experiments (PDF)

■ AUTHOR INFORMATION

Corresponding Author

*yuliu@nankai.edu.cn

ORCID

Yu Liu: 0000-0001-8723-1896

Notes

The authors declare no competing financial interest.

■ ACKNOWLEDGMENTS

We thank NNSFC (21432004, 21372128, and 91527301), and the 973 Program (2015CB856500) for financial support

■ REFERENCES

- (1) (a) Ge, Z.; Liu, S. *Chem. Soc. Rev.* **2013**, *42*, 7289–7325. (b) Zhang, P.; Cheng, F.; Zhou, R.; Cao, J.; Li, J.; Burda, C.; Min, Q.; Zhu, J.-J. *Angew. Chem., Int. Ed.* **2014**, *53*, 2371–2375.
- (2) (a) Castet, F.; Rodriguez, V.; Pozzo, J. L.; Ducasse, L.; Plaquet, A.; Champagne, B. *Acc. Chem. Res.* **2013**, *46*, 2656–2665. (b) Velema, W. A.; van der Berg, J. P.; Hansen, M. J.; Szymanski, W.; Driessen, A. J. M.; Feringa, B. L. *Nat. Chem.* **2013**, *5*, 924.
- (3) Lee, D.; Yang, S. M.; Kim, T. H.; Jeon, B. C.; Kim, Y. S.; Yoon, J. G.; Lee, H. N.; Baek, S. H.; Eom, C. B.; Noh, T. W. *Adv. Mater.* **2012**, *24*, 402–406.
- (4) (a) Bernardi, M.; Palumbo, M.; Grossman, J. C. *Nano Lett.* **2013**, *13*, 3664–3670. (b) Zhang, Q.-W.; Li, D.; Li, X.; White, P. B.; Mecinović, J.; Ma, X.; Ågren, H.; Nolte, R. J. M.; Tian, H. *J. Am. Chem. Soc.* **2016**, *138*, 13541–13550.
- (5) (a) Hinkelmann, M. V.; Virlogeux, A.; Niehage, C.; Poujol, C.; Choquet, D.; Hoflack, B.; Zala, D.; Saudou, F. *Nat. Commun.* **2016**, *7*, 13233. (b) Wang, Y. X.; Liu, Y. *Acta Chim. Sinica.* **2015**, *73*, 984–991.

- (6) (a) Uttamapinant, C.; Howe, J. D.; Lang, K.; Beránek, V.; Davis, L.; Mahesh, M.; Barry, N. P.; Chin, J. W. *J. Am. Chem. Soc.* **2015**, *137*, 4602–4605. (b) Boettiger, A. N.; Bintu, B.; Moffitt, J. R.; Wang, S.; Beliveau, B. J.; Fudenberg, G.; Imakaev, M.; Mirny, L. A.; Wu, C. T.; Zhuang, X. *Nature* **2016**, *529*, 418–422. (c) Laine, R. F.; Albecka, A.; van de Linde, S.; Rees, E. J.; Crump, C. M.; Kaminski, C. F. *Nat. Commun.* **2015**, *6*, 5980.
- (7) (a) LeVine, M. V.; Cuendet, M. A.; Khelashvili, G.; Weinstein, H. *Chem. Rev.* **2016**, *116*, 6552–6587. (b) Cheng, C.; McGonigal, P. R.; Schneebeli, S. T.; Li, H.; Vermeulen, N. A.; Ke, C.; Stoddart, J. F. *Nat. Nanotechnol.* **2015**, *10*, 547–553. (c) Kay, E. R.; Leigh, D. A. *Angew. Chem., Int. Ed.* **2015**, *54*, 10080–10088.
- (8) (a) Carr, P.; Evans, N. H.; Parker, D. *Chem. Soc. Rev.* **2012**, *41*, 7673–7686. (b) Heine, J.; Müller-Buschbaum, K. *Chem. Soc. Rev.* **2013**, *42*, 9232–9242. (c) Law, G. L.; Pham, T. A.; Xu, J.; Raymond, K. N. *Angew. Chem., Int. Ed.* **2012**, *51*, 2371–2374. (d) Isaac, M.; Denisov, S. A.; Roux, A.; Imbert, D.; Jonusauskas, G.; McClenaghan, N. D.; Sènèque, O. *Angew. Chem.* **2015**, *127*, 11615–11618.
- (9) (a) Chen, G.; Yang, C.; Prasad, P. N. *Acc. Chem. Res.* **2013**, *46*, 1474–1486. (b) Tian, J.; Zeng, X.; Xie, X.; Han, S.; Liew, O. W.; Chen, Y. T.; Wang, L.; Liu, X. *J. Am. Chem. Soc.* **2015**, *137*, 6550–6558.
- (10) (a) Jalani, G.; Naccache, R.; Rosenzweig, D. H.; Haglund, L.; Vetrone, F.; Cerruti, M. *J. Am. Chem. Soc.* **2016**, *138*, 1078–1083. (b) Parola, S.; Julián-López, B.; Carlos, L. D.; Sanchez, C. *Adv. Funct. Mater.* **2016**, *26*, 6506–6544.
- (11) Bagheri, A.; Arandiyán, H.; Boyer, C.; Lim, M. *Adv. Sci.* **2016**, *3*, 1500437.
- (12) Nakagawa, T.; Hasegawa, Y.; Kawai, T. *Chem. Commun.* **2009**, 5630–5632.
- (13) Han, M.; Zhang, H.-Y.; Yang, L.-X.; Jiang, Q.; Liu, Y. *Org. Lett.* **2008**, *10*, 5557–5560.
- (14) Ding, Z.-J.; Zhang, Y.-M.; Teng, X.; Liu, Y. *J. Org. Chem.* **2011**, *76*, 1910–1913.
- (15) (a) Kotova, O.; Daly, R.; dos Santos, C. M.; Boese, M.; Kruger, P. E.; Boland, J. J.; Gunnlaugsson, T. *Angew. Chem., Int. Ed.* **2012**, *51*, 7208–7212. (b) Chen, P.; Li, Q.; Grindy, S.; Holten-Andersen, N. J. *Am. Chem. Soc.* **2015**, *137*, 11590–11593.
- (16) (a) Steemers, F. J.; Verboom, W.; Reinhoudt, D. N.; van der Tol, E. B.; Verhoeven, J. W. *J. Am. Chem. Soc.* **1995**, *117*, 9408–9414. (b) Bünzli, J. C. G.; Pigué, C. *Chem. Soc. Rev.* **2005**, *34*, 1048–1077.
- (17) (a) Yamamoto, T.; Yagyu, S.; Tezuka, Y. *J. Am. Chem. Soc.* **2016**, *138*, 3904–3911. (b) Murray, D. J.; Patterson, D. D.; Payammyar, P.; Bholra, R.; Song, W.; Lackinger, M.; Schlüter, A. D.; King, B. T. *J. Am. Chem. Soc.* **2015**, *137*, 3450–3453.
- (18) (a) Fudickar, W.; Linker, T. *J. Am. Chem. Soc.* **2012**, *134*, 15071–15082. (b) Filatov, M. A.; Karuthedath, S.; Polestshuk, P. M.; Savoie, H.; Flanagan, K. J.; Sy, C.; Sitte, E.; Telitchko, M.; Laquai, F.; Boyle, R. W.; Senge, M. O. *J. Am. Chem. Soc.* **2017**, *139*, 6282–6285.
- (19) Tremblay, M. S.; Halim, M.; Sames, D. *J. Am. Chem. Soc.* **2007**, *129*, 7570–7577.
- (20) The corresponding control experiments of 2/3 and their discussion seeing SI.